

Experiments for a new friction stir welding (FSW) technology, to make square tubes of aluminium alloy sheets

V. Verbițchi¹, M. Vlascici², C. Ciucă¹ and I.-A. Perianu¹

¹National Research & Development Institute for Welding and Material Testing - ISIM, Timișoara, Romania

²Nano Inteliform S.R.L. Timișoara, Romania

E-mail: vverbitchi@isim.ro

Keywords

Friction stir welding (FSW), FSW equipment, FSW experiments, butt welding, square tube, aluminium alloy, sheet, steel model, FSW technology, friction stir processing (FSP), repair by FSP

1. Introduction

A new technology for friction stir welding (FSW) was developed, to make square tubes from aluminium alloy sheets. A square-section tube (40 mm x 40 mm) of S235 steel, according to EN 10025, was used as a model or pattern, on which two sheets, of 2 mm thickness, of aluminium alloy were previously bended as U shaped profiles. The wings of the U profiles were positioned without any groove, for the butt welding by FSW, to make a square tube of aluminium alloy.

Two pairs of such U-shaped profiles (each 300 mm long), bended from aluminum alloy sheets, were placed on a 600 mm long pattern made of a square steel tube.

This set-up is the test piece of four joints (marked I, II, III and IV), in the experiments for the elaboration of the new technology, as described below in this paper.

The authors of this paper consider that the proposed technology has original elements, regarding the target, technical solution, certain parameters and factors of the FSW process, for the application under consideration, compared to the references [1 - 15] and other publications.

2. Equipment

The experiments have been conducted on the multifunctional friction processing machine, type MMPF, a new experimental model contrived and made in a previous project. This is an automated and programmable machine with digital control and display for the position and movements of the tool for the following processes: friction stir welding (FSW), friction stir processing (FSP), friction drilling, deformation threading, milling and polishing. The parameters of the following drives are pre-set in the operation program: rotation and X-Y-Z translations of the tool.

The MMPF type of the multifunctional friction processing machine is equipped with brushless motors of alternating electric current, powered by inverters, equipped with adjustment, control and protection systems, integrated into the central system.

The control unit of the MMPF machine is equipped with a high-performance machine automation controller (MAC), with

software that allows the programming of the parameters for the innovative processes approached by this machine, within a control system, specific to the technologies of processing by friction, with application possibilities to other categories of processes, too.

The experimental model MMPF is used for innovative or unconventional friction-based processes, but also for conventional cutting or grinding operations. The possibilities of using this multifunctional machine in other processes were also analyzed, for example crimping.

The MMPF machine allows the execution by the mentioned processes of some test pieces, samples or parts, from aluminum alloy sheets or plates, with appropriate results. It is possible to approach other material kinds, too.

2.1. Set-up of the multifunctional friction processing machine, type MMPF

Figure 1 shows the multifunctional MMPF friction processing machine.

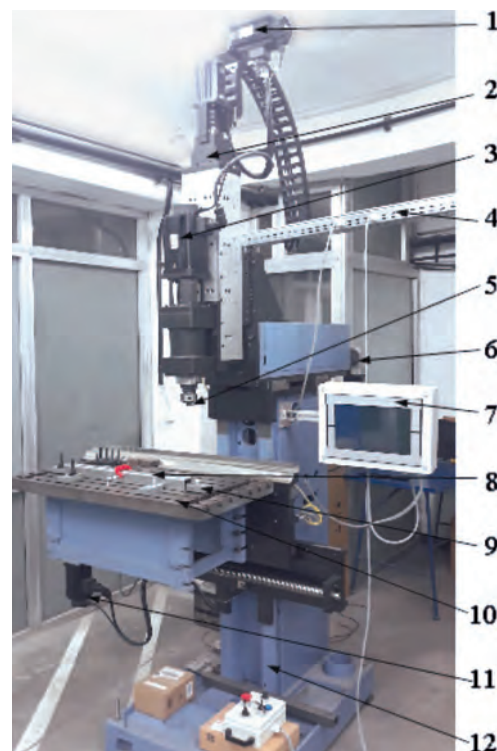


Figure 1. Multifunctional friction processing machine, MMPF type.

It was designed and executed in the J-FAST project of the MANUNET Program, as an experimental model for alternative friction processes. The technical requirements for this equipment are based on the expertise of the project partners.

The equipment complies with the quality and precision conditions of machine tools, specified in the following standards: ISO 3070-1; 2; 3: 2007 and ISO 1984-1; 2: 2001.

The operating mode is based on the MMPF machine's functional and programming menu. The components of the MMPF are as follows: 1 - Vertical translation actuator (Oz); 2 - Vertical force transducer; 3 - Servomotor for rotating friction tools; 4 - Cables to the Control unit; 5 - Friction tool; 6 - Cross motion actuator (Oy); 7 - Control panel; 8 - Parts to be joined; 9 - Fixture set (jig); 10 - Travel table; 11 - Length motion actuator (Ox); 12 - Equipment body.

2.2. Main technical characteristics

This equipment has the following main technical characteristics:

- The sizes of the table: 900 mm x 400 mm;
- Length travel stroke (X): max. 500 mm;
- Cross travel stroke (Y): max. 200 mm;
- Vertical translation stroke (Z): max. 300 mm;
- Vertical thrust force (Z): max. 20 kN;
- Horizontal advance force (X): max. 10 kN;
- Rotation speed of the friction tool (for: friction stir welding-FSW, friction stir processing- FSP, friction drilling-FD, friction threading-FT, friction riveting-FR, milling-M and grinding- G): 5- 3450 rpm ;
- Power of the servomotor for the rotation of the friction tools: 5 kW;
- Adjustable travel speed in the range: 0 - 2000 mm / min.

3. Experiments

Four joints were executed, with the marks I, II, III and IV. The experiments performed are described below, with some explanations regarding the position of the FSW test pieces or samples, the selection of tools and parameters, the execution of the FSW test joints, the interpretation of the results, etc.

Figure 2 shows the positioning of the joining test piece, on the table of the MMPF equipment.

A quenched FSW tool, own-made of C 45 grade steel, EN 10083, as well as tools of sintered tungsten carbide have been used for these joining tests.

The joining parameters are mentioned for each experiment. The run of each joining process is described and the FSW test welds are presented.

In Table 1, the characteristics of the tools used for experiments are presented.

Table 2 presents the parameters used for all FSW or FSP passes (or runs) applied for the execution of the joints I, II, III

Table 1. Characteristics of the FSW tools

Material	Pin type and length	Pin diameter [mm]	Shoulder type / diameter	Tool clamping diameter
Steel C45; quenched	Flat tronconic pin; 1.5 mm	Large diameter Φ 2.5; Small diameter Φ 2.0	Flat / Φ 14	Φ 22
Sintered tungsten carbide powder (in previous tests only)	Flat tronconic pin; 1.85 mm	Large diameter Φ 3.80; Small diameter Φ 3.6	Flat / Φ 22	Φ 22

and IV of the joining test piece for making a square tube, out of aluminum alloy sheets.

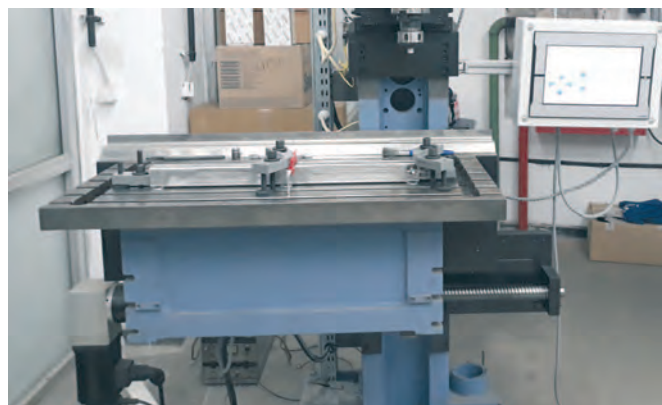


Figure 2. Positioning of the test piece for both FSW and FSP on the table of the MMPF machine.

Some of the butt welds presented length flaws, as channels behind the FSW tool. These welds were repaired by means of post-weld passes of the tool over the same weld. This repair method is an application of the friction stir processing (FSP), a variant of FSW. The repair processing needed a few processing tests of the parameters, carried out on other zones of the U-shaped sheets of aluminium alloy.

3.1. Execution of the mark I joint

Figure 3 illustrates the insertion of the parameter "Welding depth", with the use of an additional caliber, for the commands "Read welding start" and "Read welding end", on the command panel.

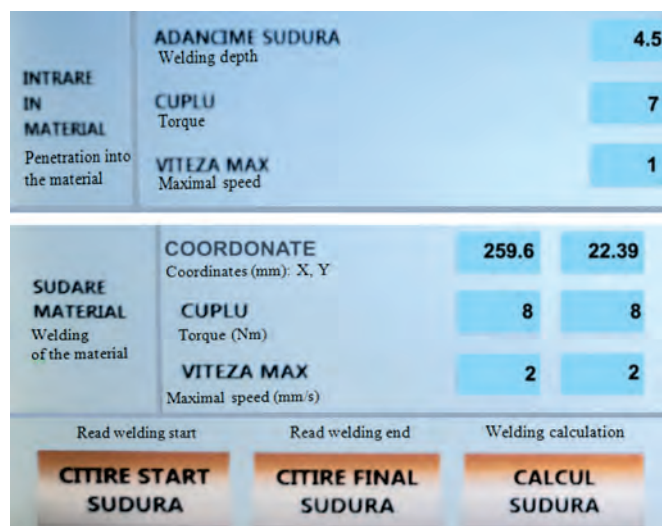


Figure 3. Inserting the parameter "Welding depth", with the use of an additional caliber, for the commands "Read welding start" and "Read welding end", on the command panel.

Table 2. The parameters of all FSW and FSP passes (or runs) applied for the execution of the joints I, II, III and IV of the joining test piece for making a square tube, out of aluminum alloy sheets.

Number	Joint mark	Weld mark	Pin penetration H(weld) [mm]	Rota- tional speed n [rpm]	Travel speed v(x) [mm/s]	Advance force F(x) [kN]	Path correction force F(y) [kN]	Thrust force F(z) [kN]	Temperature (final, after 7-10 sec) [°C]	Equipment/ Process type All MMPF, except FSW (4-10)
1	I	1.1	1.7	1000 999	2 1.93	-0.51 -0.06	-1 -0.95	0.47 0.52		FSW
2	I	1.2	1.75	1400	2					FSP
3	I	1.3	1.8	2199 2202 2202 2199	1.01 0.97 0.98 0.99	0.19 0.42 0.27 0.35	-0.2 -0.19 -0.17 -0.18	0.78 0.86 0.82 0.81	102- 104 (long pass)	FSP
4	I	1.4	1.85	2205 2195	1.02 1.0	0.27 0.53	-0.14 -0.14	1.04 1.04	59-60 (short pass)	FSP
5	II	1	1.65	1200	1.67					FSW (-4-10)
6	II	2	1.7 Related to II.1	2202 2199 2200 2196 2205 2202	1.03 1.0 1.01 1.01 1.02 0.99	0.46 0.45 0.49 0.47 0.33 0.45	-0.3 -0.29 -0.31 -0.3 -0.3 -0.29	1.05 1.01 1.15 1.12 1.02 1.02	121-122	FSP
7	III	III.1	1.60	1000	0.83					FSW (-4-10)
8	III	9.1	1.7 Zero level defined by welding start reading before each run	1994 2002 2001 1994 2004 2000 2001 2002	1.02 0.94 1.0 1.02 0.99 0.98 1.04 1.03	0.51 0.29 0.20 0.21 0.25 0.40 0.46 0.17	-0.26 -0.27 -0.28 -0.28 -0.29 -0.28 -0.27 -0.27	1.3 1.4 1.31 1.28 1.29 1.36 1.26 1.23	103	FSP
9	III	9.2	1.7	2100	0.99				160-200	FSP
10	III	9.3	(1.55); 1.7 Interrupted; continued	2097 2103	1.02 0.96	0.28 0.41	-0.33 -0.32	0.96 1.22	103	FSP
11	III	9.4	1.6	2200 2200 2200	0.90 0.90 0.91	0.20 0.44 0.36	-0.22 -0.23 -0.22	1.33 1.24 1.17	59- 60	FSP
12	IV	8.1	1.7	2000	1				64 - 67	FSW
13	IV	8.2	1.7	2000	1				74- 77	FSP
14	IV	8.3	1.7	2000	1				50- 53	FSP
15	IV	8.4	1.70 constant	1999 2001 1999 2001 2000 2002 1999 2000	1.01 1 0.99 1 1 1 1 0.99	0 0.17 0.32 0.36 0.22 -0.1 -0.13 0.18	-0.27 -0.26 -0.27 -0.28 -0.27 -0.28 -0.28 -0.27	1.44 1.45 1.42 1.39 1.37 1.32 1.29 1.26	102-103	FSW

For programming the welding path, the FSW tool is driven by manual commands to the start point of the expected weld, so that the tool pin touches the base metal; in this position, the virtual button “Read welding start” must be touched. Next, the FSW tool is driven by manual commands to the end point of the intended weld, so that the tool pin touches the base metal; in this position, the virtual button “Read welding end” must be pressed. Then, the virtual button “Welding calculation” must be pressed. In this situation, the welding path is stored.

The depth of penetration into the base metal of the FSW tool pin is pre-set in the “Welding depth” section of the “Welding parameters” screen on the control panel (touch screen) of the MMPF; the value resulting from the following relationship is entered:

$$H(weld) = H(pin) + H(shoulder) \tag{1}$$

wherein

- $H(weld)$ is the “Welding depth”;

- $H(\text{pin})$ is the length of the pin; for the tool used here, $H(\text{pin}) = 1.5 \text{ mm}$;
- $H(\text{shoulder})$ is the depth of penetration of the FSW tool shoulder into the base metal; the recommended value used here is $H(\text{shoulder}) = 0.2 \text{ mm}$.

With these values, "Welding depth" results as follows:

$$H(\text{weld}) = 1.5 + 0.2 \quad (2)$$

$$H(\text{weld}) = 1.7 \text{ mm} \quad (3)$$

The depth of penetration into the base metal of the FSW tool pin can also be pre-set using an additional caliber. In this case, under the "Welding depth" section of the "Welding parameters" screen on the control panel (touch screen) of the MMPF, the value resulting from the following relationship must be entered:

$$H(\text{weld} + \text{addition}) = H(\text{pin}) + H(\text{shoulder}) + H(\text{addition}) \quad (4)$$

where, $H(\text{addition})$ is the thickness of the additional caliber; in this case, $H(\text{addition}) = 2.8 \text{ mm}$.

With these values, "Welding depth" results in the following value:

$$H(\text{weld} + \text{addition}) = 1.5 + 0.2 + 2.8 \quad (5)$$

$$H(\text{weld} + \text{addition}) = 4.5 \text{ mm} \quad (6)$$

The use of an add-on caliber has the advantage that the check of the welding rout can be done before welding, but without touching the base metal. This check is done if $H(\text{weld}) = 0$ is pre-set and the additional caliber is removed from under the tool pin. After this verification, "Welding depth" is pre-set again at the value $H(\text{weld} + \text{addition})$, and then the welding is performed.

Table 2 shows sampled values collected from the instant X-Y-Z coordinates of the FSW tool motion, the components of the force, the components of the travel speed and the rotational speed of the tool, by the execution of the FSW 1.1 pass (or run) of the mark I joint, as well as of the subsequent passes.

Figure 4 presents the execution by FSW of the welding (or pass) 1.1 of the mark I joint.



Figure 4. Execution by FSW of the welding (pass) 1.1 of the mark I joint.

Further, the passes (or runs) 1.2, 1.3 and 1.4 of the mark I test joint have been executed by FSP. The results of the experiments are analyzed in the chapter 4 of this paper.

3.2. Execution of the mark II joint

Figure 5 shows a snapshot of instant values from the coordinates of a position, the force components, the travel speed components and the rotational speed of the tool, by the execution of the FSP 2 pass (run), to improve the initial FSW joint, at the joint having the mark II.

WELDING		SUDURA		
Axis	Position	Force	Speed	Rotary speed
	POZITIE (MM)	FORTA (KN)	VITEZA [mm/s]	TURATIE RPM
AXA X	478.89	0.45	0.99	2202
AXA Y	29.67	-0.29	0	
AXA Z	251.39	1.02	0	

Figure 5. Sample of the instant values from the position coordinates, components of force, components of travel speed and rotational tool speed, by the execution of the FSP 2 pass, to improve the initial FSW joint, at the mark II joint.

Figure 6 shows the execution by FSP of the pass (run) 2, for the remediation of the initial FSW welding, at the joint with the mark II.



Figure 6. Execution by FSP of the pass 2, to improve the initial FSW welding, at the joint with mark II.

Pass 2, executed by FSP, was performed to improve the initial FSW weld that had short channels on the middle line, because of low temperature during the process, at the mark II joint.

Figure 7 shows the mark II joint, with the initial FSW weld (covered), improved by the FSP II.2 pass, after the execution.

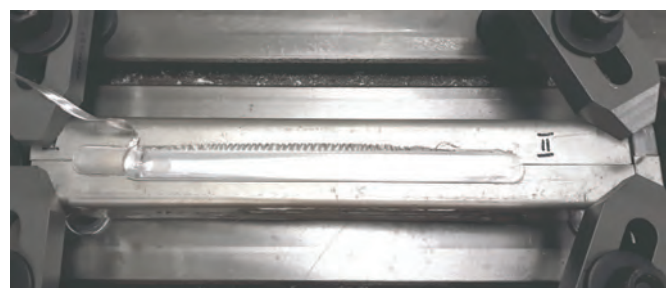


Figure 7. Mark II joint, with the initial FSW welding (covered), improved by the FSP II.2 pass, after the execution.

The results of the experiments are analyzed in the chapter 4 of the paper.

3.3. Execution of the mark III joint

Figure 8 presents the appearance of the FSW welding with mark III, initially executed.

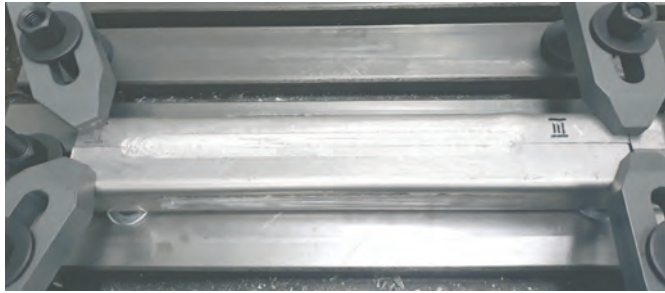


Figure 8. Appearance of FSW welding with mark III, initially executed.

The FSW parameters from the initial FSW welding are listed in Table 2.

Depending on the requirements and the possibilities of multi-clamping, for fixing the sheets to be joined, as well as for closing the gap between these sheets, the joints made by FSW or FSP passes could only be executed on shorter segments, than the whole joining path. This caused the disadvantage to obtain lower temperature values, which led to some cavity defects on certain zones. Under such conditions, by the FSP passes (runs) 9.1, 9.2, 9.3 and 9.4, some local imperfections of the FSW joint with mark III, initially executed, were corrected.

By the execution of the pass FSP 9.2 of the joint III, the chip (also called burr, collar or flash, in English) is continuous and has a larger thickness, by the action of the tool's shoulder on the base metal, through which the heat for the plasticization of the base metal is generated. Due to the large thickness (0.20 - 0.25 mm), the temperature of the base metal behind the FSW tool was in the range 160 - 200 °C, higher than by other passes. Thus, the results of this run are better.

Figure 9 shows the execution of FSP 9.4 pass, over the FSP 9.3 run, on the mark III joint.



Figure 9. Execution of the FSP 9.4 pass, over the FSP 9.3 run, of the mark III joint.

The FSP 9.4 pass is executed over the previous run FSP 9.3, to close the channel following the pin. For this purpose, the position of the tool for the initial Y coordinate is pre-set so that the left flank of the channel is tangentially aligned to the small diameter of the tool pin (at its bottom). Thus, if the tool pin rotates clockwise, the pin drives the metal taken from the flank of the channel to the center of the channel, to close it up.

Figure 10 shows the appearance of the passes FSP 9.1 – FSP 9.4, for the improvement of the initial FSW-made weld with mark III. The appearance of the passes is appropriate. No surface imperfections are observed. The channel behind the pin, in the area of the final hole from the FSP 9.3 pass was closed, by executing the FSP 9.4 pass.

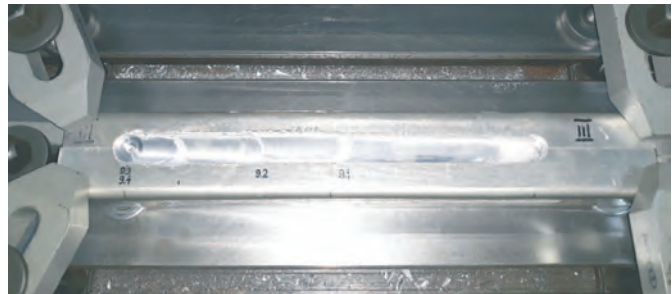


Figure 10. Appearance of the FSP 9.1 – FSP 9.4 passes, to improve the initial FSW-made weld with mark III.

3.4. Execution of the mark IV joint

Figure 11 shows the appearance of passes (or runs) 8.1 and 8.4 executed by FSW, respectively the appearance of passes (runs) 8.2 and 8.3 executed by FSP, from the mark IV joint.

We observe the three vises that perform the tightening on the cross direction, related to the welding direction. This favors the joint execution and avoids cavity, channel or tunnel defects behind the FSW tool. The vises are located at short distances from each other, which requires the FSW or FSP passes to be executed on short zones, with the corresponding disadvantages. It should also be noted that the vertical clamps are also placed, which secure the sheets to the square tube steel pattern, preventing local metal deformation and strain in the elastic range. These deformations and elastic returns can cause deviations from the required values of some parameters. For example, the penetration depth can neither be set, nor achieved at the required value, because of elastic deformations.

Another factor that can adversely affect the results is the slipping of the base metals, because of insufficient force in the vises and clamps. One solution to this is to fasten with screws the sheets or parts to be welded, onto the machine table. However, this depends on the shape and sizes of the parts to be joined.

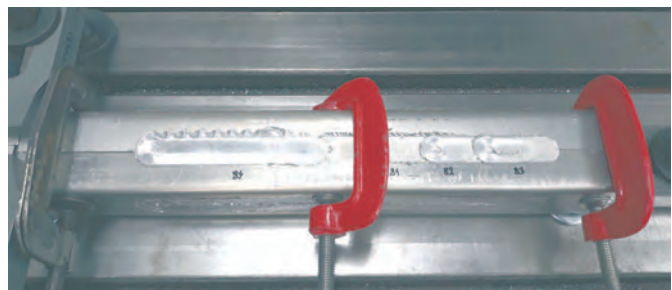


Figure 11. Appearance of the passes (or runs) 8.1 and 8.4 executed by FSW, respectively the aspect of the passes (runs) 8.2 and 8.3 executed by FSP, of the mark IV joint.

4. Results

In the Figure 12, the 45 mm x 45 mm square tube (as a test piece) in exposed, welded on the generator line by FSW and FSP, of aluminum alloy sheets with steel core, in the final stage.



Figure 12. The 45 mm x 45 mm square tube (test piece) welded by FSW and corrected by FSP, on the generator line, made of aluminum alloy sheets with steel core, in the final stage.

4.1. Metallographic analysis

From the FSW joining test pieces, on which the FSP was also applied, as described in the previous chapters, specimens were taken for metallographic examination on the cross section to the welding and processing direction.

Macroscopic metallographic examination was performed according to SR EN ISO 17639: 2014, SR EN 1321: 2000, SR EN ISO 25239-5: 2011 and PS-LIEA-03-04. The imperfections were identified and examined according to SR EN ISO 6520-1 and SR EN ISO 25239-5: 2011.

The results of the macroscopic metallographic examination are described below.

Figure 13 shows the specimen with mark 1.2, taken from the joining test piece IV. The appearance is appropriate. In the middle area there are traces of stirring and mixing of the base metals, from which the weld metal was formed. Below the processed surface, there is a slight delimitation of two layers of the weld metal, as a result of the FSP passes. The penetration depth of the FSW tool shoulder into the base metals is estimated to be approximately 0.25-0.30 mm. This is not considered a lack of material, in the case of FSW. No imperfections are detected. This FSW joint is accepted for a mean execution level of a manufacturing standard.

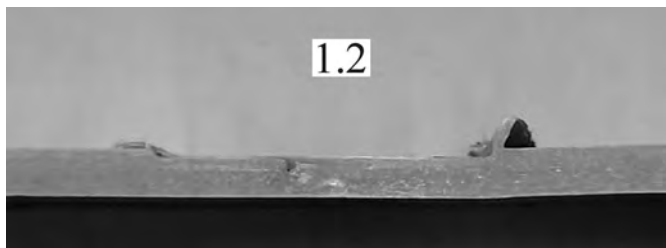


Figure 13. Specimen 1.2 (Joining test piece IV). Macroscopic metallographic examination.

The specimen with mark 1.3, taken from the joining test piece I, does not have a proper appearance. In the middle area we can see the traces of stirring the base metals, which did not materialize in a compact and uniform mixture of the base metals. Only a very weak delimitation of two weld metal layers is seen under the processed surface, as a result of the successive FSP passes. The penetration depth of the FSW tool shoulder in the base metals is estimated to be about 0.31-0.37 mm, larger than in the specimen 1.2. A round shaped cavity imperfection with a size of approximately 1.12 mm is observed, which can only be accepted for a low manufacturing level.

The specimen with mark 2.1, taken from the joining test piece II, has an appropriate appearance. In the middle area there are

traces of stirring and mixing of the base metals, from which the compact metal of the weld was formed. Near the processed surface, there is a delimitation of two weld metal states, as a result of the FSP passes. The penetration depth of the FSW tool shoulder into the base metals is approximately 0.32-0.38 mm, which is relatively large and explains the proper running of the FSP process. A small imperfection, as a cavity of 0.96 mm with rounded edges is seen, which can be accepted for a middle level execution of a manufacturing specification.

Figure 14 shows the specimen with mark 2.2, taken from the joining test piece III. The appearance is appropriate. In the middle area, some traces are seen of proper stirring and mixing of the base metals, which formed the compact metal of the weld. Below the processed surface, there is no obvious delimitation in weld metal states as a result of FSP passes. The thermo-mechanically influenced zone, with favorable effect in FSP, is clearly observed. The penetration depth of the FSW tool shoulder in the base metals is approximately 0.24-0.28 mm, which is adequate. The proper running of the FSP passes is also explained by the uniformity of the z coordinate of the surface of the base metal sheets, during the process. A very small imperfection, as a cavity of about 0.15 mm x 0.25 mm with rounded edges was detected, which can be allowed. This FSW joint is accepted for a medium quality level of a manufacturing standard.

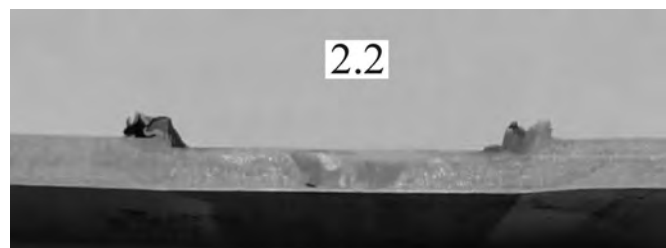


Figure 14. Specimen 2.2 (Joining test piece III). Macroscopic metallographic examination.

4.2. Influences of the parameters

The rotational speed of the FSW tool is one of the main parameters of both the FSW and FSP processes. This speed range was $n = 999 - 2205$ rpm, for all passes or runs performed in the experiments. The heat developed by the FSW and FSP processes is directly proportional to the rotational speed.

The technological advance speed on the X direction (feed rate) is the other main parameter. The technological advance speed had values in the range $v = 0.83 - 2.0$ mm/s. The heat developed by the FSW and FSP processes is inversely proportional to the feed rate of the tool.

A very important positioning parameter is the depth $H(\text{weld})$ of the tool's penetration into the base metal, defined by the relationships (1) - (6) of the first part of this work. A higher value of the penetration increases the frictional force of the tool's shoulder with the base metal, which contributes to obtaining a higher value of the linear energy developed by the friction process, by the higher amount of heat developed in the unit of time. The thin chip (also called collar, burr or flash) of the FSW has a thickness that can be measured relatively accurately and represents a check of the depth of penetration of the tool's shoulder into the base metal. The thickness of the base metal is reduced by removing the chip, but this reduction of thickness must be limited due to the requirements regarding the piece

being executed. Therefore, the thickness of the chip, equal to the depth of penetration of the FSW tool shoulder into the base metal is limited to 0.20 - 0.25 mm. This means that the maximum penetration depth of the tool into the base metal was limited to a maximum of 1.70 - 1.75 mm.

The experiments performed confirmed that, for higher values of the penetration depth, the appearance and structure of the FSW and FSP passes are appropriate.

The MMPF machine, on which the mentioned FSW and FSP tests were carried out, allows the positioning and driving of the FSW tool with high precision, due to the digital technology used in the adjustment and control systems of the MMPF machine. But these features of the mentioned machine are not enough. It is necessary for the surface of the base metal to be absolutely flat, without uneven zones or distortions, which change the depth of effective penetration of the tool shoulder, respectively it leads to structural defects and improper appearance. Thus, in order to obtain adequate results, the clamping and fastening of the parts to be joined by FSW or processed by FSP must be carried out as accurately as possible, so they do not allow any mounting gaps or deformations of the parts by positioning or during the FSW and FSP processes.

The force components in the X direction have values in the range $F(x) = -0.51 \dots +0.53$ kN. This is the force that drives the tool to advance through the material, to ensure the continuity of the stirring and mixing process of the base metal, in order to form the weld metal (by FSW), respectively the processed metal (by FSP). The force F_x is variable, because it is the actuation quantity of the control system that maintains the technological advance speed $v(x)$. The $F(x)$ force also has negative or braking values, if the $v(x)$ speed exceeds the set value, due to the too high acceleration in the immediately preceding phase. Force $F(x)$ has positive acceleration values, if the velocity $v(x)$ is below the set value, due to frictional forces, which caused a too high deceleration in the immediately preceding phase. The inertia of the tool drive block also has an effect in this control process.

The force components in the Y direction have values in the range $F(y) = -0.12 \dots -1.0$ kN. This is the force acting on the tool to do the necessary corrections to compensate for the deviations in the Y direction from the path to the X direction. The values are exclusively negative in this case, which means that the deviations from the path are in one way, produced by the stress caused by the reactions of the forces with which the tool pin acts on the base metal. A component of the weight of the FSW tool drive block can also cause this stress, if there are mounting gaps in the X-Y-Z travel guides.

The force components in the Z direction have values in the range $F(z) = +0.47 \dots +1.45$ kN. This is the force acting on the tool as the actuator quantity in the control system of the tool position on the O_z axis, from which the depth of penetration of the tool's shoulder into the base metal depends. But this control system cannot remove the effect of the base metal unevenness. Lower values of the $F(z)$ force result in a lower pressure of the tool on the base metal, and thus the depth of penetration of the tool's shoulder into the base metal will be reduced, in order to maintain the set depth. Higher values of the force $F(z)$ result in a greater pressing of the tool on the base metal, and thus the depth of penetration of the tool's shoulder into the base metal will be increased to maintain the set depth.

The forces with which the tool's pin acts on the base metal have also a role, by vector summation, on each component of

the force with which the tool (consisting of the shoulder and pin) acts on the base metal. A similar statement applies to the tool's shoulder.

The components of the force acting on the base metal are order 2 or indirect parameters, which are not directly set, but they represent actuating quantities of the MMPF machine control systems.

The temperature of the base metal during the process is also a parameter of order 2, which cannot be directly set, but it is achieved through the main parameters: the rotational speed of the tool and the speed of movement, but also the depth of penetration. The temperature is directly proportional to the rotational speed of the tool, respectively, the temperature is inversely proportional to the speed of movement in the X direction. In addition, the temperature is proportional to the depth of penetration, according to a more difficult relationship.

The temperature achieved on each pass was measured with a thermocouple connected to the associated multimeter. Measurements were done at 20 - 30 mm behind the tool, during the welding process. In the final crater area, the final temperature value was measured, approximately 7 - 10 seconds after the completion of the FSW or FSP process. The operating mode applied required this interval to prepare the measurement. These values are listed in Table 2.

Preheating was not used with the analyzed joining test pieces. The initial temperature of the base metal was approximately equal to the room temperature, at which the FSW test welds were performed, in the case of the first FSW passes. At the following passes, the initial temperature was 2-5 °C higher, considering that the breaks between the passes were of the order of a few minutes, preparation of the operations being necessary: cleaning the previous pass, mounting the fastening parts, positioning the tool, reading the welding start, reading the welding end, weld calculation, path verification, prescribing the depth of penetration, rotational speed, travel speed, as well as other parameters and factors.

In contrast, if the next FSW or FSP pass is made after a maximum of one minute after the completion of a considered pass, the temperature of the base metal at the beginning point of the next FSW or FSP pass may be only 30-40 °C lower than that at the final moment of the considered pass. This means that the preheating is higher, if the temperature is higher at the end of the considered pass for comparison and the brake is shorter.

The use of a preheating method leads to appropriate results. A recommended method for this purpose is the application of the hybrid FSW-WIG process, where the WIG electric arc performs the preheating of the base metal in front of the FSW tool, up to a temperature of 400 - 500 °C, depending on the parameters of the WIG process, but also on the distance between the WIG electric arc and the FSW tool.

Several measurements were made along the welding route, behind the tool. It has been found that the temperature varies approximately linearly, from the value of the room temperature at the start point to the maximum value at the end point of the weld. Preheating or using the FSW- WIG process has the potential to increase the efficiency and performance of the proposed technology.

The short length passes (70 - 90 mm) had lower temperature values: 57 - 70 °C. In contrast, the longer passes (160 - 180 mm) recorded higher temperature values, namely: 103 - 200 °C. All temperature values are below the recommended values of

minimum 450 - 480 °C. There are some available resources in order to increase the linear energy of the FSW and FSP processes applied for this technology, in order to increase the temperature during the process: increasing the rotational speed of the FSW tool up to 3500 rpm; reducing the travel speed to 0.5 mm/second; achieving optimum penetration depth; reducing heat loss; preheating, etc.

The most appropriate result, regarding the appearance and structure of the whole joining test piece is the FSP 2 pass from the II joint. The related parameters are selected as appropriate parameters, which lead to appropriate results.

The FSP 8.4 pass from the IV joint has a proper appearance and adequate structure, as well. The parameters of this pass are also considered as appropriate parameters, with appropriate results.

The appearance of the FSW welds is appropriate. Some of these welds have been improved by FSP. The visual examination and the metallographic analysis show that the FSW joints of the aluminum alloy sheets are adequate, as there is no gap between the welded ends of the aluminum alloy sheets. No flaws beyond limits were detected. Allowed imperfections are the final holes after lifting the FSW tool and two channels with the length of 8-12 mm behind the tool, at the FSW test piece mark I, caused by insufficient side tightening of the sheets, which can be corrected. The final holes are understood and accepted in the current stage of this FSW technology. When defining the final stage of this technology and the applications, the final hole must be removed outside the joints, depending on the possibilities of using the clamps, vises and other fixing parts.

There is a gap between the aluminum alloy sheets and the steel tube wall, used as a pattern in this case. This gap depends on both the FSW tool and parameters. Depending on this gap, the steel tube model can be later extracted from the aluminum alloy tube or it can be kept inside, as a tough core of increased strength.

Conclusions

The depth of penetration into the base metal must be greater than 0.2 mm, so that the frictional force releases sufficient heat to plasticize the base metal, so that the base metal is properly stirred and mixed, to form the metal of the FSW joint.

In the case of FSP, the same finding is valid, but the penetration depth must be limited, so that it does not reduce excessively the thickness of both the base metal and the weld.

The temperature of the base metal during the welding process ranged from the room temperature value of 18 °C to 200 °C. These temperature values are relatively low for the plasticization. There are resources for increasing the temperature, by the following means: increasing the rotational speed of the FSW tool up to 3500 rpm; reducing the travel speed to 0.5 mm/second; increasing the depth of penetration up to 0.30 mm; using tools with a larger diameter of the shoulder up to $\Phi 22$ mm; using preheating; reducing heat losses by isolation, proper design of the parts to be welded, adequate position, etc.

The FSP 2 pass of the mark II joint has the proper appearance and structure of the processed weld. The parameters from this pass (FSP processed pass) are considered appropriate:

$H(\text{weld})$ (pre-set) = 1.7 mm; n (pre-set) = 2200 rpm; n (measured) = 2196-2205 rpm; $v(x)$ (pre-set) = 1.0 mm/s; $v(x)$ (measured) = 0.99-1.03 mm/s; $F(x)$ (measured) = 0.33...0.49 kN; $F(y)$ (measured) = - 0.29...- 0.31 kN; $F(z)$ (measured) = 1.01...1.15 kN; t (measured) = 121-122 °C.

The pass of FSP 8.4 of the mark IV joint has also proper appearance and structure of the processed weld. The parameters from this pass (FSP processed pass) are considered appropriate: $H(\text{weld})$ (pre-set) = 1.7 mm; n (pre-set) = 2000 rpm; n (measured) = 1999-2002 rpm; $v(x)$ (pre-set) = 1.0 mm/s; $v(x)$ (measured) = 0.99-1.01 mm/s; F_x (measured) = - 0.13 ... 0.36 kN; $F(y)$ (measured) = - 0.26 ... - 0.28 kN; $F(z)$ (measured) = 1.26 ... 1.45 kN; t (measured) = 102-103 °C.

Adequate preparation of the parts to be welded, mechanization and automation assure repeatability and quality. The target applications are structure elements for devices, appliances, tools, welded structures or automobiles. The involved areas of the applications are: manufacturing, electro-technique and automotive industries, as well as construction activities.

Acknowledgement

This article is based on results of the project with the title "A rapid joint by alternative processes", acronym J-FAST, in the frame of the Program Manunet, financed by the Local Funding Program GAITEK of the Basque Country, Spain, respectively the Executive Unit for Financing the Higher Education, Research, Development and Innovation - UEFISCDI of Romania, by the Contracts no.17 and no.18 of the period 2015 – 2017.

References

- [1]. W.M. Thomas, E.D. Nicholas, J.C. Needham, M.G. Murch, P. Temple-Smith and C.J. Dawes, "Friction-stir butt welding", GB Patent No. 9125978.8, International patent application No. PCT/GB92/02203, (1991).
- [2]. C.B. Fuller, "Friction Stir Tooling: Tool Materials and Designs", Friction Stir Welding and Processing, ASM International, (2007), pag.7-37.
- [3]. W. J. Arbogast, "Friction Stir Welding: After a Decade of Development", Weld. J., vol.85, March (2006), pag.28-35.
- [4]. K. Kimapong and T. Watanabe, "Lap Joint of A5083 Aluminum Alloy and SS400 Steel by Friction Stir Welding", Materials Transactions 46 (4) (2005), pag. 835-841.
- [5]. S. Chimbli; Dana Medlin and W. Arbogast: "Minimizing Lack-of-Consolidation Defects in Friction Stir Welds". In the volume "Friction Stir Welding and Processing IV", edited by R.S. Mishra, and others, pages 135-143. The Minerals, Metals & Materials Society, TMS. TMS Annual Meeting, Orlando, Florida, USA, 2007. P 978-0-87339-661-5.
- [6]. L.N. López de Lacalle; G. Urbikain Pelayo; I. Azkona; J. M. Pérez; V. Verbičchi; R. Cojocar; L.N. Boțilă; C. Ciucă and I.A. Perianu: "Making steel – aluminium joints by fast alternative processes". In the journal "SUDURA (Welding)", ISSN 1453-0384, Issue 1, April, (2017), year XXVII, pages 5-13. Conference "SUDURA 2017", Iasi, April 6th-7th (2017), organized by ASR / Romanian Welding Society.
- [7]. L.-N. Boțilă; R. Cojocar and C. Ciucă: "Friction stir processing in multiple passes of the cast aluminum alloy EN AW 4047 (AlSi12)". BID-ISIM – Welding and Material Testing, nr. 2/2019, pag.13-17, ISSN 1453-0392.
- [8]. L.-N. Boțilă; R. Cojocar and C. Ciucă: "Friction stir processing in multiple passes of the ENAW 5083(AlMg4,5Mn0,7) cast aluminum alloy". BID-ISIM – Welding and Material Testing, nr.3/2019, pag.3-7, ISSN 1453-0392.

- [9]. L.-N. Boțilă; R. Cojocaru and C. Ciucă: "New ecologic method for joining of titanium alloys". BID-ISIM – Welding and Material Testing, nr.3/2019, pag.19-26, ISSN 1453-0392.
- [10]. C. Ciucă, R. Cojocaru; L.-N. Boțilă and I.-A. Perianu: "General considerations regarding friction stir welding of some steels used in important industrial fields". The 10th International Conference Innovative Technologies for Joining Advanced Materials. November 7th - 8th, 2019, Timisoara, Romania.
- [11]. R. Cojocaru, C. Ciucă, L.-N. Boțilă, V. Verbițchi and I.-A. Perianu: Program Partnerships in priority areas. Project 219/ (2014-2017). "Innovative, ecological and efficient joining technologies of metallic and polymeric materials used in the automotive industry, using the friction stir welding technique", Acronym "Inova-FSW".
- [12]. R. Cojocaru; L.N. Boțilă; C. Ciucă; H. Dașcău and V. Verbițchi: "Friction Stir Lap Welding of Light Alloy Sheets". The 10th International Conference "Structural Integrity of Welded Structures", July 11th-12th, (2013), Timisoara, Romania. Proceedings of the Conference. Published by TTP

- Trans Tech Publications Ltd., Pfaffikon, Switzerland, (2013). ISSN print 1022-6680. Pages187-193.
- [13]. L.-N. Boțilă; R. Cojocaru; C. Ciucă: "Characteristics of friction stir welding tools for high hardness materials". TIMA 11. The 5th International Conference "Innovative technologies for joining advanced materials". Timisoara, Romania, 2011. Proceedings CD, pages 8.
- [14]. L.-N. Botila; R. Cojocaru; V. Verbitchi; et al.: Project PN 19 36 01 01. "Researches regarding the development of new innovative methods of applying the friction stir welding (FSW) process, in order to extend the possibilities of application in priority areas (within the Laboratory for Friction Stir Processing, FSP). Stage 3. "Experimental verification of the application technique of FSW welding in inert gas environment. Referential finalization". ISIM Timisoara, 2019-2020.
- [15]. *** EN ISO 25239:2011 - "Friction stir welding - Aluminium", Part 4: "Specification and qualification of the welding procedure". Part 5: "Quality requirements and inspection".



Professional training programme

International Welding Engineer	
part. I	21.09 - 02.10.2020
part. II	19.10 - 27.11.2020
part. III	11.01 - 29.01.2021

International Welding Inspection Personnel - Comprehensive Level	
part. I	09.11 - 27.11.2020
part. II	11.01 - 29.01.2021

International Welding Inspection Personnel - Standard Level	
part. I	12.11 - 27.11.2020
part. II	14.01 - 29.01.2021

International Welding Inspection Personnel - Basic Level	
part. I	12.11 - 27.11.2020
part. II	18.01 - 29.01.2021

International Welded Structures Designer	
part. I	19.10 - 06.11.2020
part. II	15.01 - 29.01.2021

International Welding Specialist	
part. I	21.09 - 14.10.2020
part. II	11.01 - 29.01.2021

Polyethylene Welding Operator		
course	authorization	reauthorization
1	11.06 - 17.06.2020	18.06 - 19.06.2020
2	05.11 - 11.11.2020	12.11 - 13.11.2020

Non - Destructive Examination Operators Level 1+2, acc. to SR EN ISO 9712	
visual	21.09 - 25.09.2020
penetrant liquids	14.09 - 18.09.2020
magnetic particles	28.09 - 02.10.2020
ultrasounds	12.10 - 30.10.2020
penetrant radiation	09.11 - 27.11.2020

e-mail: isim@isim.ro

Additional information:

- *International level training & Polyethylene welding*
Dr.eng. Marius Cocard,
tel. +40 256-491831 int. 182
fax: +40 256-492797
e-mail: isim@isim.ro
- *Non-destructive examination*
Ing. Marius Oproiu,
tel.: +40 256-491831 int. 161
fax: +40 256-492797
e-mail: isim@isim.ro

ISIM offer is also available on the SICAP public procurement platform (e-licitatie.ro)